THE JOURNAL OF BIOLOGICAL CHEMISTRY VOL. 291, NO. 46, pp. 23854–23868, November 11, 2016

Bone-protective Functions of Netrin 1 Protein*

Received for publication, May 17, 2016, and in revised form, September 16, 2016 Published, JBC Papers in Press, September 28, 2016, DOI 10.1074/jbc.M116.738518

Kenta Maruyama[‡1], Takahiko Kawasaki[§], Masahide Hamaguchi[¶], Motomu Hashimoto[‖], Moritoshi Furu[‖], Hiromu Ito[‖], Takao Fujii[‖], Naoki Takemura[**], Thangaraj Karuppuchamy[‡], Takeshi Kondo[‡], Takumi Kawasaki[‡], Masahiro Fukasaka[‡], Takuma Misawa[‡], Tatsuya Saitoh[‡ ‡‡], Yutaka Suzuki[§§], Mikaël M. Martino[‡¶¶], Yutaro Kumagai[‡], and Shizuo Akira[‡‖‖2]

From the Laboratories of [‡]Host Defense and [¶]Experimental Immunology, World Premier Institute (WPI) Immunology Frontier Research Center (IFReC) and the [‖‖]Research Institute for Microbial Diseases, Osaka University, Osaka 565-0871, Japan, the [§]Division of Brain Function, National Institute of Genetics, 1111 Yata, Mishima 411-8540, Japan, the [‖]Department of the Control for Rheumatic Diseases, Graduate School of Medicine, Kyoto University, Kyoto 606-8507, Japan, the [**]Division of Innate Immune Regulation, International Research and Development Center for Mucosal Vaccine, Institute for Medical Science, The University of Tokyo, 4-6-1 Shirokanedai, Minato-ku, Tokyo 108-8639, Japan, the [‡‡]Department of Inflammation Biology, Institute for Enzyme Research, Tokushima University, 3-18-15 Kuramoto-cho, Tokushima 770-8503, Japan, the [§§]Departments of Functional Genomics and Medical Genome Sciences, Graduate School of Frontier Sciences, The University of Tokyo, 5-1-5 Kashiwanoha, Kashiwa, Chiba 277-8562, Japan, and the [¶¶]European Molecular Biology Laboratory, Australian Regenerative Medicine Institute, Monash University, Victoria 3800, Australia

Edited by Amanda Fosang

Netrin 1 was initially identified as an axon guidance factor, and recent studies indicate that it inhibits chemokine-directed monocyte migration. Despite its importance as a neuroimmune guidance cue, the role of netrin 1 in osteoclasts is largely unknown. Here we detected high netrin 1 levels in the synovial fluid of rheumatoid arthritis patients. Netrin 1 is potently expressed in osteoblasts and synovial fibroblasts, and IL-17 robustly enhances netrin 1 expression in these cells. The binding of netrin 1 to its receptor UNC5b on osteoclasts resulted in activation of SHP1, which inhibited VAV3 phosphorylation and RAC1 activation. This significantly impaired the actin polymerization and fusion, but not the differentiation of osteoclast. Strikingly, netrin 1 treatment prevented bone erosion in an autoimmune arthritis model and age-related bone destruction. Therefore, the netrin 1-UNC5b axis is a novel therapeutic target for bone-destructive diseases.

Rheumatoid arthritis (RA)[3] is a serious bone-destructive disease caused by an autoreactive immune system. Generally, RA is characterized by proliferating synovial fibroblasts, severe joint inflammation, and bone erosion, accompanied by hyperactivated bone-degrading osteoclasts (1), large multinucleate cells that differentiate from the macrophage lineage (2). Both osteoblasts and synovial fibroblasts express the RANK ligand (RANKL) and M-CSF. The stimulation of myeloid precursors by these cytokines activates several transcription factors, including nuclear factor of activated T cells, cytoplasmic calcineurin-dependent 1 (NFATc1) (3), Jun dimerization protein 2 (Jdp2) (4, 5), the cellular oncogene Fos (c-Fos) (6), and nuclear factor κB (NF-κB) (7). In RA, IL-17-producing Th17 cells act as osteoclastogenic T cells by producing RANKL themselves (8), which suggests that they are the major trigger of the excessive osteoclastogenesis in RA. Among the osteoclastogenic proteins induced by RANKL, ATP6v0d2, Sbno2, and DC-STAMP are essential for multinucleation, as the respective knock-out mice cannot form large multinucleated osteoclasts and exhibit mild osteopetrosis (9–11). However, the expression of osteoclast differentiation markers in these knock-out mice is normal, suggesting that osteoclast multinucleation is critically involved in bone degradation (9–11).

Denosumab, a monoclonal antibody directed against RANKL, blocks osteoclast differentiation and is thus highly effective in the treatment of RA and osteoporosis (12, 13). However, recent studies have described adverse effects in patients

* This research was supported by the Cabinet Office, Government of Japan, and the Japan Society for the Promotion of Science (JSPS) through the Funding Program for World-Leading Innovative R&D on Science and Technology (FIRST Program), a research fellowship from the JSPS for the Promotion of Science for Young Scientists, a grant from the Osaka University MEET project, a grant from the Astellas Foundation for Research on Metabolic Disorders, a scholarship from the Naito Foundation Natural Science, a visionary research grant from Takeda Science Foundation, a KAKENHI grant-in-aid for Challenging Exploratory Research, a KAKENHI grant-in-aid for Young Scientists A, grants from the Japan Intractable Diseases Research Foundation and the SENSHIN Medical Research Foundation, a Senri Life Science Foundation Kishimoto grant, and grants from Nouchi Shitagau, Japan Prize Foundation, Mochida Memorial, and Japan Rheumatism Foundation. The authors declare that they have no conflicts of interest with the contents of this article.

[1] To whom correspondence may be addressed: Laboratory of Host Defense, WPI Immunology Frontier Research Center (IFReC), Osaka University, 3-1 Yamadaoka, Suita, Osaka 565-0871, Japan. Tel.: 81-6-6879-8303; Fax: 81-6-6879-8305; E-mail: maruyama@biken.osaka-u.ac.jp.

[2] To whom correspondence may be addressed: Laboratory of Host Defense, WPI Immunology Frontier Research Center (IFReC), Osaka University, 3-1 Yamadaoka, Suita, Osaka 565-0871, Japan. Tel.: 81-6-6879-8303; Fax: 81-6-6879-8305; E-mail: sakira@biken.osaka-u.ac.jp.

[3] The abbreviations used are: RA, rheumatoid arthritis; OA, osteoarthritis; BMP, bone morphogenic protein; CAIA, collagen antibody-induced arthritis; CIA, collagen-induced arthritis; μCT, micro computed tomography; MSC, mesenchymal stem cell; OM, osteoclast medium; RANKL, receptor activator of nuclear factor κ-B ligand; TRAP, tartrate-resistant acid phosphatase; ALP, alkaline phosphatase; CREB, cAMP-response element-binding protein; MDM, monocyte-derived macrophage; qPCR, quantitative real-time PCR; FAK, focal adhesion kinase; ITIM, immunoreceptor tyrosine-based inhibitory motif; SIRPα, signal regulatory protein α; PIR-B, paired immunoglobulin-like receptor B; p, phospho; h, human.

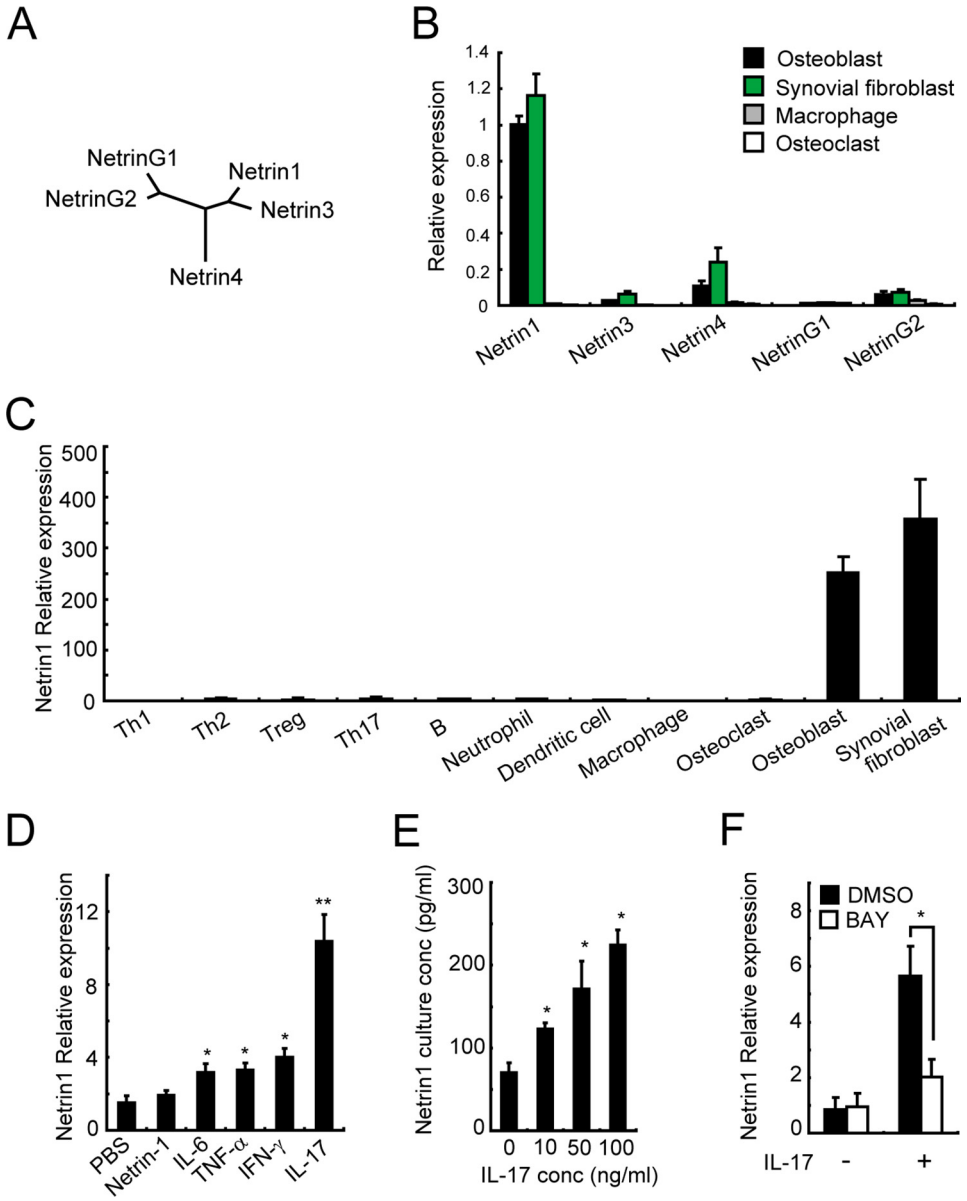

FIGURE 1. **Netrin 1 expression.** *A*, phylogenetic tree of the netrin family of proteins, including netrin 1. *B* and *C*, mRNA levels of the netrin family genes (*B*) and netrin 1 in various cell types (*C*). *Treg*, regulatory T cell. *D*, netrin 1 mRNA levels in cytokine-stimulated calvarial osteoblasts. The cells were harvested 6 h after stimulation with 200 ng of cytokine/ml. *E*, netrin 1 protein levels measured in the supernatants of calvarial osteoblasts stimulated with 200 ng of IL-17/ml for 16 h. *conc*, concentration. *F*, netrin 1 expression in calvarial osteoblasts treated with 200 ng of IL-17/ml for 4 h in the presence or absence of 5 mM BAY117085 (*BAY*), an NF-κB inhibitor. *Error bars*, S.E.; *, $p < 0.05$, **, $p < 0.01$ ($n = 3$).

administered Denosumab, including infection, hypocalcemia, and osteonecrosis of the jaw (14). Regulating the inhibition of osteoclast multinucleation may circumvent these adverse effects. Although the movement of osteoclast precursors, facilitated by increased actin polymerization, is a critical factor in the multinucleation step of osteoclast formation (15), the soluble factor that regulates this process has yet to be identified.

Netrin 1 is an axon guidance cue that mediates the attraction and repulsion of neural axons by regulating cytoskeletal rearrangements (16–19). The determinant of these variable functions is the expression of netrin 1 surface receptor UNC5b on neural cells. Generally, the expression of this receptor mediates the repulsion of neural axons, whereas expression of another netrin 1 receptor, DCC, results in neuronal attraction (20). It has been reported that netrin 1 also inhibits monocyte migration (21, 22) by modifying the cytoskeleton of myeloid cell types. Furthermore, a previous study indicated that netrin 1 is expressed in human osteoblastic cells (23). These observations prompted us to explore whether netrin 1 also regulates osteoclast multinucleation.

Results

Netrin 1 Is Expressed in Osteoblasts and Synovial Fibroblasts—To identify the netrin 1-producing cell population in the osteoimmune system, we examined netrin 1 expression in various hematopoietic and mesenchymal cell types. In mammals, three secreted netrins, netrin 1, netrin 3, and netrin 4, and two glycosylphosphatidylinositol-linked netrins, netrin G1 and netrin G2, have been reported (Fig. 1*A*). We found that netrin 1 is highly expressed in osteoblasts and synovial fibroblasts (Fig.

1*B*) but is barely detectable in T cells, B cells, neutrophils, dendritic cells, macrophages, and osteoclasts (Fig. 1*C*). When osteoblasts were stimulated with various cytokines, IL-17 was the most potent inducer of netrin 1 expression among the cytokines typically elevated in RA (Fig. 1, *D* and *E*). Furthermore, IL-17-induced netrin 1 expression in osteoblasts was NF-κB-dependent (Fig. 1*F*).

To extend our findings to human RA, we examined the synovial fluid of RA patients (Fig. 2, *A* and *B*) and found that, when compared with the synovial fluid from osteoarthritis (OA) patients, it contained significantly higher levels of IL-17 and netrin 1 (Fig. 2*B*). We also found a significant correlation between the concentrations of IL-17 and IFN-γ in the synovial fluid of RA but not OA patients (Fig. 2, *C* and *D*). In RA synovial fluid, there was correlation between netrin 1 and the IL-17 concentration (Fig. 2*D*). These data suggest that netrin 1 is induced in RA joints in an IL-17-dependent manner.

Netrin 1 Inhibits Osteoclast Multinucleation—In RA patients with high netrin 1 concentrations, the levels of the bone destruction marker human type 1 collagen cross-linked C-terminal telopeptide (CTXI) were relatively low (Fig. 2*E*). In the synovial fluid of OA patients, the netrin 1 concentration correlated negatively with that of CTXI (Fig. 2*F*), whereas in the synovial fluid of these patients and those with RA, there was no correlation between CTXI and IL-17 concentration (Fig. 2*G*). These results prompted us to explore the *in vivo* role of netrin 1 during osteoclast formation. First, because netrin 1 deficiency is lethal, we analyzed the bones of netrin 1 gene knock-out mice beginning on embryonic day 19. Histological analysis of the metaphyseal portion of the tibia showed that these netrin 1 gene-deficient mice had decreased trabecular bone accompanied by marked increases in osteoclast number and nuclei (Fig. 3, *A*–C). In contrast, adult mice heterozygous for netrin 1 gene exhibited normal bone volumes and osteoclast parameters (Fig. 3, *D*–*F*). We then examined the *in vitro* effect of netrin 1 on osteoclastogenesis and found that, in the presence of RANKL, netrin 1 inhibited osteoclast multinucleation (Fig. 3, *G*–*I*). Other than netrin 1, osteoblasts produce osteoclast inhibitory axon guidance factors such as Sema3A (24), EphB4 (25), and netrin 4 (26). A comparison of these axon guidance factors showed that netrin 1 was the most potent inhibitor of osteoclastogenesis (Fig. 3*J*). Both apoptosis and TRAP activity were normal in netrin 1-stimulated osteoclasts (Fig. 3, *K* and *L*), but these cells had significantly fewer resorption pits than untreated cells (Fig. 3, *M* and *N*). The netrin 1-related decrease in the number of resorption pits in the netrin 1-treated osteoclasts correlated with the reduction in multinucleated cells, but the areas of the pits/osteoclast areas in these and the control cells were similar (Fig. 3, *M* and *N*). Thus, although netrin 1-treated osteoclasts are functionally normal, a fusion defect in these cells results in fewer resorption pits. Osteoblast-derived axon guidance factors such as Sema3A (24) and EphB4 (25) are local mediators of osteoclast and osteoblast functions and, as bidirectional regulators, may contribute to bone remodeling. We therefore explored whether netrin 1, as an osteoblast-derived axon guidance factor, had an effect on osteoblastogenesis (Fig. 4, *A*–*E*). In calvarial osteoblasts cultured with increasing netrin 1 concentrations, there was no effect on bone nodule formation or the expression of osteoblast differentiation markers such as ALP, Runx2, RANKL, and osteoprotegerin (OPG) (Fig. 4, *A*–*E*). We also examined the expression levels of osteoclast-derived osteoblast inducers ("clastokines") in netrin 1-treated osteoclasts and found an induction of bone morphogenetic protein (BMP)-2 expression (Fig. 4*F*). Thus, to test the hypothesis that netrin 1-induced BMP-2 released from osteoclasts influences osteoblastogenesis, calvarial cells were cultured in a concentrated culture supernatant from netrin 1-stimulated osteoclasts. This osteoclast medium (OM) significantly enhanced bone formation and mineralization when compared with OM from osteoclasts not treated with netrin 1 (Fig. 4, *G* and *H*). Additionally, BMP-2 neutralizing antibody attenuated the osteogenic effect of OM from netrin 1-treated osteoclasts (Fig. 4, *G* and *H*). To gain insight into the transcriptional regulation of BMP-2 by netrin 1, we examined the occupancy of the BMP-2 promoter by CREB, a pivotal BMP-2 transcription factor (27). Indeed, CREB binding to the BMP2 promoter was increased after netrin 1 stimulation (Fig. 4*I*). In CREB knockdown osteoclasts, however, netrin 1-induced BMP-2 expression was abolished (Fig. 4*J*). These data indicate that the netrin 1-CREB axis in osteoclasts induces BMP-2 expression, which in turn stimulates bone formation. Taken together, our findings suggest that netrin 1 does not affect osteoblast differentiation directly, but it may stimulate bone formation by a mechanism involving osteoclasts.

Netrin 1 Inhibits VAV3-RAC1 Signaling via the UNC5b Receptor—To gain further insight into the molecular mechanism of the netrin 1-induced inhibition of osteoclast formation, we analyzed netrin 1 signaling and its cross-talk with RANKL signaling. The possibility that the altered expression of RANK and Csf1R (colony-stimulating factor 1 receptor) is responsible for the inhibition of multinucleation in netrin 1-treated osteoclasts was excluded by the finding that their levels were similar after netrin 1 or PBS treatment (Fig. 5*A*). Because neural cells contain five netrin 1 surface receptors (UNC5a, UNC5b, DCC, Neo1, and Adora2b), we examined receptor expression on osteoclasts. Both UNC5b and Adora2b were detected at high levels (Fig. 5*B*). UNC5b knockdown MDMs gave rise to significantly more and larger osteoclasts than control shRNA-transduced osteoclasts (Fig. 5, *C* and *D*), whereas Adora2b knockdown had no effect on netrin 1-induced osteoclast inhibition (data not shown). In co-cultures of UNC5b knockdown MDMs and calvarial osteoblasts, osteoclast numbers were slightly increased after 7 days (Fig. 5*E*). These data indicated that UNC5b is a *bona fide* netrin 1 receptor in osteoclasts.

To evaluate the effects of netrin 1 on RANKL-induced osteoclast differentiation, the expression of various osteoclastogenic genes was examined by quantitative real-time PCR (qPCR) (Fig. 5*F*). At every time point, expression of the genes encoding NFATc1, c-Fos, Jdp2, TRAF6, TRAP, DC-STAMP, β3-integrin, and ATP6v0d2 was similar in netrin 1-treated and PBS-treated osteoclasts (Fig. 5*F*). In a study measuring the activation of NFATc1 in response to RANKL, we found that netrin 1 treatment did not alter the binding of NFATc1 to their target promoter regions (Fig. 5*G*). Netrin 1 also had no effect on

A RA

age	sex	hNetrin1(pg/ml)*	hIL17 (pg/ml)*	hIFNγ (IU/ml)*	CTXI (pg/ml)*	Bisphosphonate	Biologics	MTX(mg/w)	PSL(mg/day)	ESR(mm/h)	DAS28-ESR	Operation
64	♀	245.322	4.95864	0.109774	359.8764	–	CTLA4-Ig (abatacept)	8.0	6.5	20	4.12	TKA
70	♀	378.378	0	0.203866	252.7621	–	–	0.0	0.0	48	ND	TKA
62	♀	407.484	3.30576	0.282276	620.9834	–	–	4.0	0.0	3	2.45	TKA
60	♀	478.17	41.322	0.297958	392.9654	+	–	14.0	4.0	14	ND	TKA
70	♀	536.328	24.24224	0.282276	501.3254	–	–	0.0	0.0	32	4.19	TKA
84	♀	548.856	14.87592	0.250912	670.2834	+	–	2.0	2.5	29	5.84	TKA
69	♀	577.962	15.97784	0.250912	277.5431	–	–	6.0	2.0	110	3.99	TEA
76	♀	673.596	9.91728	0.203866	575.8743	+	–	0.0	0.0	24	4.10	TKA
85	♀	686.07	6.06056	0.109774	661.2534	+	–	0.0	2.0	ND	ND	–
65	♂	873.18	93.6632	0.39205	529.9764	–	anti TNFa-Ab (remicade)	8.0	0.0	4	3.14	TEA
80	♀	993.762	23.14032	0.125456	267.4387	–	–	0.0	0.0	95	6.06	TEA
78	♀	1097.712	8.81536	0.23523	215.9427	–	–	0.0	0.0	115	6.48	THA
43	♀	1168.398	27.548	0.360686	476.9843	–	–	8.0	2.5	8	ND	–
56	♀	1176.714	43.52584	0.219548	135.8977	–	–	0.0	0.0	88	6.27	–
53	♀	1230.768	132.2304	0.658644	283.8872	–	–	0.0	7.0	52	5.95	–
51	♀	1230.768	17.07976	0.39295	100.6542	+	–	12.0	5.0	37	6.89	TKA
53	♀	1268.19	100.2747	0.376368	330.1986	–	–	0.0	7.0	51	5.94	–
43	♀	1276.506	40.22008	0.266594	525.7643	–	–	10.0	2.5	4	ND	–
78	♀	2062.368	79.8892	0.188184	100.6542	–	–	8.0	5.0	30	4.04	TKA
60	♀	2274.426	185.6735	0.517506	356.6647	+	–	14.0	4.0	12	3.63	–

OA

age	sex	hNetrin1(pg/ml)*	hIL17 (pg/ml)*	hIFNγ (IU/ml)*	CTXI (pg/ml)*	Bisphosphonate	Biologics	MTX(mg/w)	PSL(mg/day)	Operation
76	♀	174.636	0	0.141138	224.8298	+	–	0.0	0.0	–
76	♀	191.268	11.0192	0.109774	329.2401	–	–	0.0	0.0	TKA
67	♀	282.744	9.91728	0.266594	61.08864	–	–	0.0	0.0	TKA
62	♀	286.902	3.85672	0.376368	105.0652	–	–	0.0	0.0	TKA
75	♀	303.534	2.20384	0.407732	340.4927	–	–	0.0	0.0	TKA
69	♀	332.64	3.85672	0.250912	482.9777	–	–	0.0	0.0	TKA
82	♀	382.536	4.40768	0.54887	310.6817	–	–	0.0	0.0	TKA
79	♂	382.536	2.7548	0.109774	398.1339	–	–	0.0	0.0	–
70	♂	419.958	10.46824	0.595916	170.3502	–	–	0.0	0.0	TKA
75	♂	432.432	3.30576	0.23523	413.9085	–	–	0.0	0.0	TKA
73	♂	449.064	7.71344	0.297958	325.5089	–	–	0.0	0.0	TKA
70	♂	469.854	7.16248	0.15682	306.9989	–	–	0.0	0.0	TKA
83	♀	498.96	7.16248	0.266594	359.4476	–	–	0.0	0.0	–
74	♀	523.908	9.91728	0.282276	114.6686	–	–	0.0	0.0	–
82	♀	553.014	65.01328	0.109774	45.70712	–	–	0.0	0.0	TKA
77	♀	561.33	6.61152	0.360686	259.9727	–	–	0.0	0.0	TKA
87	♀	619.542	3.85672	0.125456	36.55757	–	–	0.0	0.0	TKA
74	♀	702.702	41.87296	0.188184	61.08864	–	–	0.0	0.0	TKA
81	♀	715.176	18.73264	0.439096	197.3287	–	–	0.0	0.0	TKA
70	♀	785.862	9.36632	0.188184	147.1574	–	–	0.0	0.0	TKA

* : concentrations in synovial fluid
ND: not determined

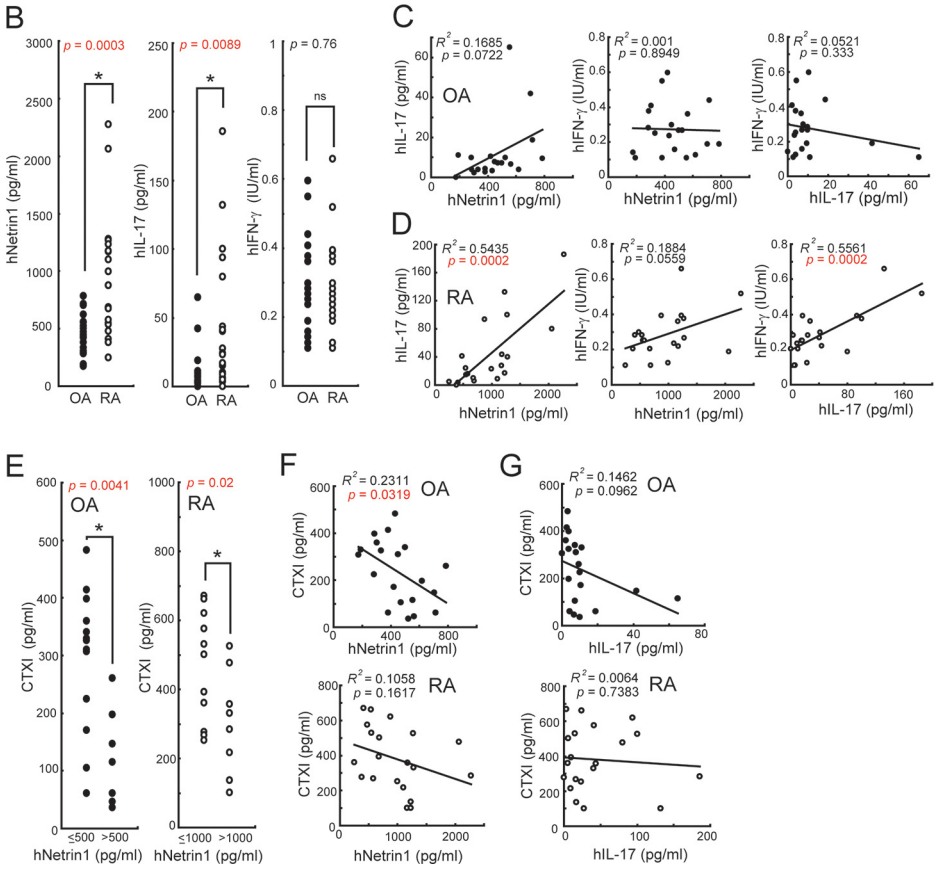

FIGURE 2. **Netrin 1 concentrations in synovial fluid.** *A*, characteristics of the RA and OA patients. *MTX*, methotrexate; *PSL*, prednisolone; *ESR*, erythrocyte sedimentation rate; *DAS*, Disease Activity Score. *TKA*, total knee arthroplasty; *THA*, total hip arthroplasty; *TEA*, total elbow arthroplasty. *B*, concentrations of human netrin 1 (*hNetrin 1*), IL-17 (*hIL-17*), and IFN-γ (*hIFN-γ*) in the synovial fluid of OA and RA patients. *ns*, not significant. *C* and *D*, correlation between hIL-17 and hnetrin 1, hIFN-γ and hnetrin 1, and hIFN-γ and hIL-17 in the synovial fluid of OA (*C*) and RA (*D*) patients. R^2 values of Pearson's product moment correlation and *p* values are shown. *E*, human CTXI concentrations in the synovial fluid of OA and RA patients. *F*, correlation between CTXI and hnetrin 1 in the synovial fluid of OA and RA patients. R^2 values of Pearson's product moment correlation and *p* values are shown. *G*, correlation between CTXI and hIL-17 in the synovial fluid of OA and RA patients; *, $p < 0.05$ ($n = 20$).

calcium oscillations induced by RANKL (Fig. 5*H*). These observations suggest that osteoclast multinucleation, but not osteoclast differentiation, is suppressed by netrin 1.

Because the formation of actin belts (Fig. 6*A*) and actin rings (Fig. 6, *B* and *C*) was dramatically impaired in the netrin 1-treated osteoclasts, we next examined the role of netrin 1

in cytoskeletal rearrangement during osteoclast formation. Because actin dynamism is predominantly regulated by the Rho GTPase RAC1 and the adhesion kinase FAK, we first quantified the activated GTP-bound form of RAC1 and phosphorylated FAK (Fig. 6, *D* and *E*). The results showed a dramatic inhibition of the RANKL-induced activation of RAC1 (Fig. 6*D*) and FAK (Fig. 6*E*) by netrin 1 treatment. In addition, constitutively active RAC1 expression partially rescued the osteoclast multinucleation defect in netrin 1-treated cells (Fig. 6, *F* and *G*). Collectively, these data showed that impaired RAC1 activation is responsible for the fusion defect in netrin 1-treated osteoclasts. Next, given the role of VAV3, a Rho GTPase nucleotide exchanger, in osteoclast multinucleation and RAC1 activation (15), we measured the levels of phosphorylated VAV3 in netrin 1-treated osteoclasts (Fig. 6*H*). In response to RANKL, VAV3 phosphorylation was significantly impaired by netrin 1 (Fig.

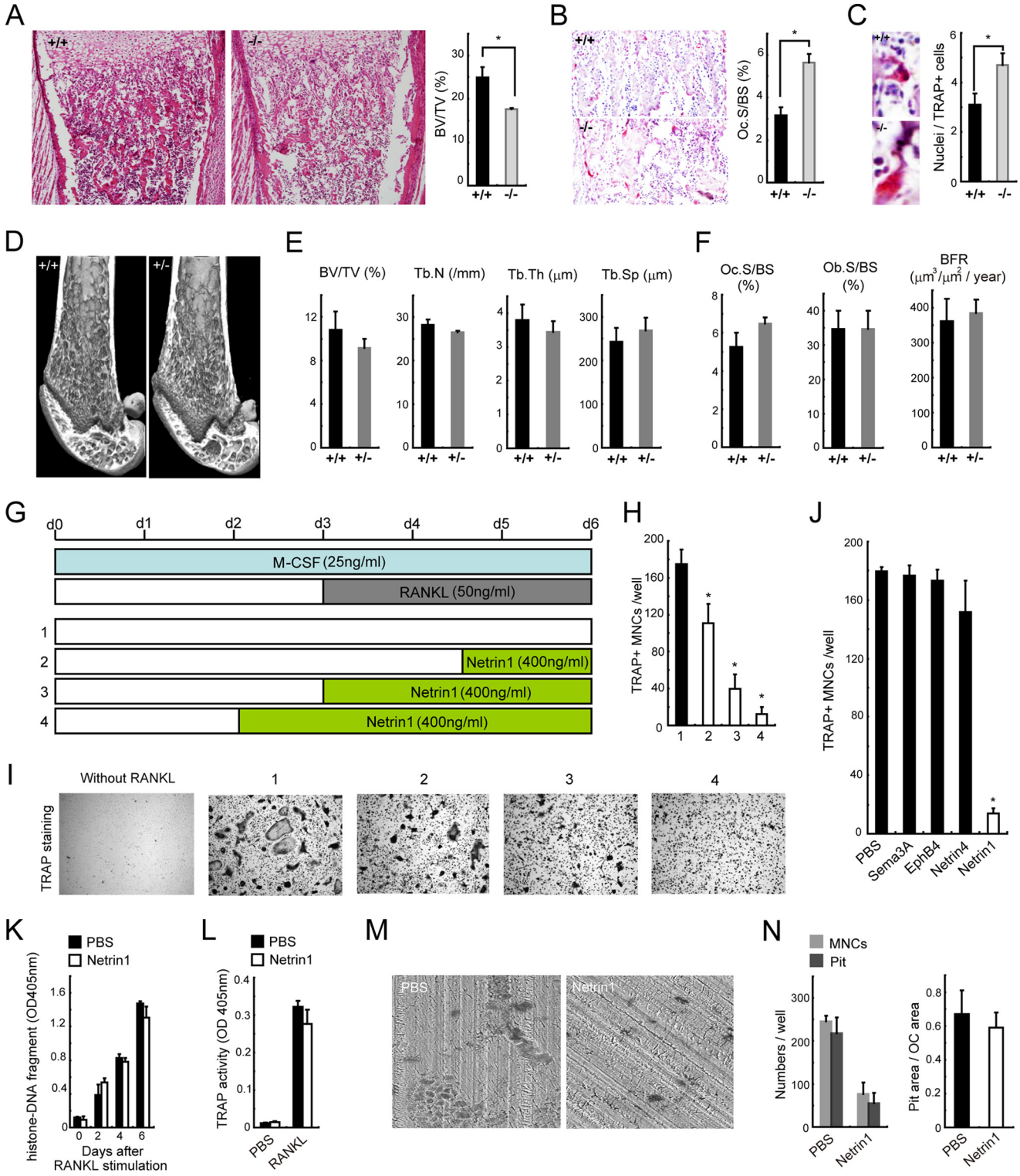

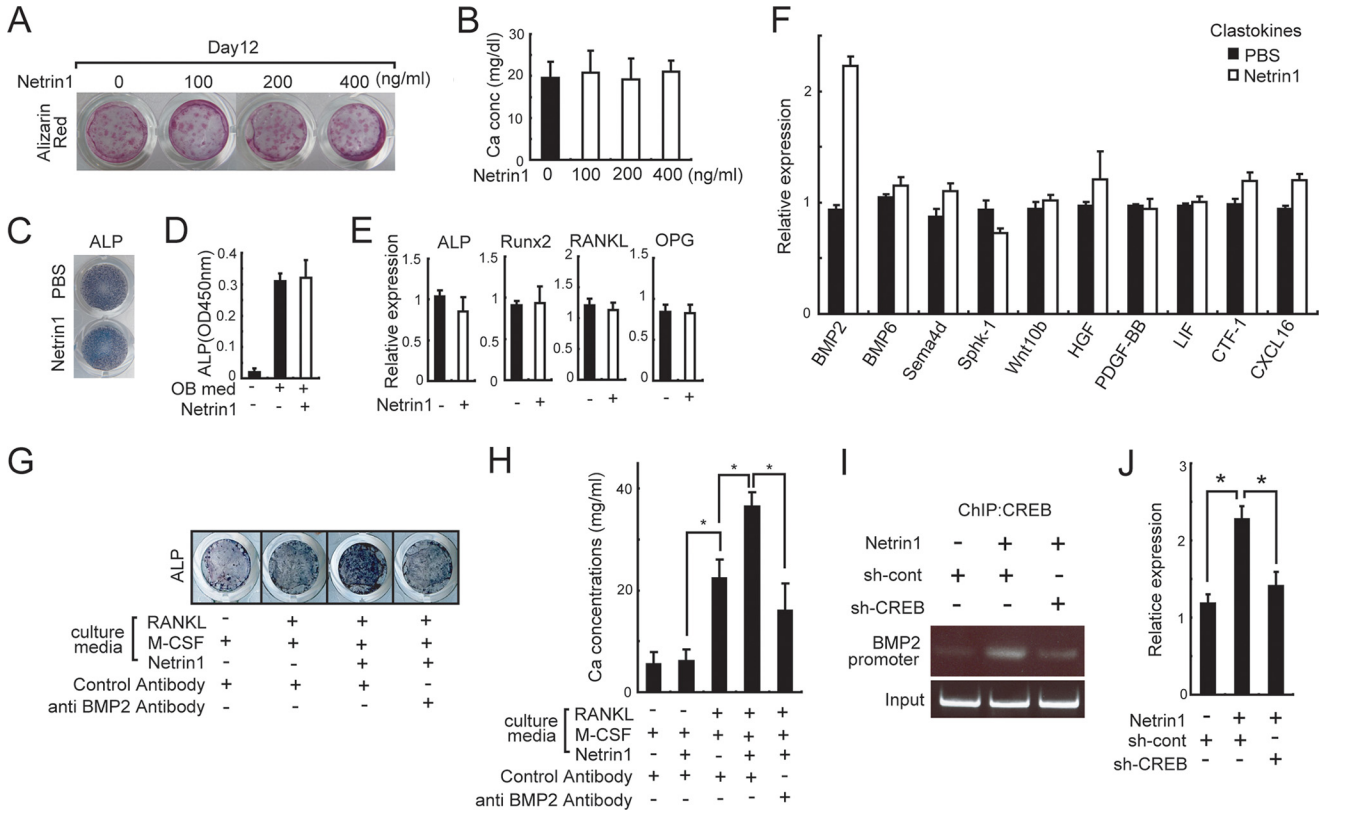

FIGURE 4. **Netrin 1-stimulated osteoclast enhances bone formation.** *A–E*, calcified nodules (*A*) and calcium concentrations (*Ca conc*) (*B*) in calvaria-derived cells treated for 12 days with an osteoblast-inducing reagent and the indicated concentrations of netrin 1 ($n = 3$). *C* and *D*, representative ALP staining images (*C*) and activities (*D*) in calvaria-derived cells treated for 12 days with an osteoblast-inducing reagent together with 400 ng of netrin 1/ml. ($n = 3$). *OD*, optical density; *OB med*, osteoblast medium. *E*, qPCR analysis of osteoblastic genes in the cells in *C* ($n = 3$). *F*, clastokine expression in netrin 1-treated osteoclasts ($n = 3$). *G* and *H*, calvarial cells cultured in osteoclast medium (see "Experimental Procedures") supplemented with 2 μM β-glycerophosphate and 2 μM ascorbic acid. An anti-BMP2 or a control antibody was added to the cultures. After 12 days, the cells were fixed, stained for ALP (*G*), and their calcium concentrations were measured (*H*). *Error bars*, S.E.; *, $p < 0.05$ ($n = 4$). *I* and *J*, ChIP analysis of cell using a CREB antibody to determine the effect of CREB knockdown (*sh-CREB*) on the induction by BMP-2 of MDMs stimulated with 60 ng of RANKL/ml plus 400 ng of netrin 1/ml. Lysates were prepared from cells treated as shown. DNA fragments of the BMP-2 promoter region were detected by PCR (*I*). *sh-cont*, sh-control. *J*, qPCR determination of BMP2 expression in *I*. *Error bars*, S.E.; *, $p < 0.05$ ($n = 5$).

6*H*). Furthermore, the RANKL-induced phosphorylation of SHP1, a phosphatase of the VAV family, was significantly enhanced in netrin 1-treated MDMs (Fig. 6*I*). Further, the knockdown of SHP1 in MDMs significantly rescued the osteoclast inhibitory effect of netrin 1 (Fig. 6, *J* and *K*).

Recently, it has been reported that immunoreceptor tyrosine-based inhibitory motif (ITIM)-harboring receptors, such as CLM-1 (28), SIRPα (29), and PIR-B (30), negatively regulate osteoclast multinucleation via a mechanism involving SHP1 activation. In netrin 1-treated osteoclasts, the expression of these receptors was slightly but significantly increased (Fig. 6*L*). These findings imply that netrin 1 inhibits VAV3-RAC1 signaling via the UNC5b-SHP1 axis (Fig. 6*M*).

Netrin 1 Prevents Bone Destruction in Arthritis—Based on our finding that netrin 1 is a potent inhibitor of osteoclast multinucleation, we explored the therapeutic potential of recombinant netrin 1 in CIA. Type II collagen was injected into 6-week-old mice, followed by a booster immunization 3 weeks later. The mice were then intravenously injected with netrin 1 or PBS (Fig. 7*A*). Netrin 1 failed to reduce the clinical scores, hind paw thicknesses, or serum proinflammatory cytokine levels of CIA mice (Fig. 7, *B*, *C*, and *F*), but it did significantly lower

FIGURE 3. **Netrin 1 inhibits osteoclast formation.** *A*, *left*, images of the hematoxylin- and eosin-stained tibias of embryonic day 19 mice deficient in netrin 1. *Right*, bone volume per tissue volume (*BV/TV*) of the mice; *, $p < 0.05$ ($n = 3$). *B*, *left*, representative images of TRAP-stained netrin 1-deficient bone. *Right*, osteoclast surface/bone surface (*Oc.S/BS*) of the mice; *, $p < 0.05$ ($n = 3$). *C*, *left*, representative images of TRAP-stained osteoclast in netrin 1-deficient bone. *Right*, number of nuclei per TRAP-positive cell in the metaphyseal portion of the tibia. *Error bars*, S.E.; *, $p < 0.05$. *D–F*, representative μCT images (*D*) and bone morphometric analysis (*E*) of the distal femurs of 7-week-old mice heterozygous in netrin 1 (ICR background). *F*, bone histomorphometric analysis of the metaphyseal portions of the tibia of these mice. $n = 3$, *BV/TV*, bone volume per tissue volume; *Tb.N*, trabecular bone number; *Tb.Th*, trabecular bone thickness; *Tb.Sp*, trabecular bone spacing; *Oc.S/BS*, osteoclast surface per bone surface; *Ob.S/BS*, osteoblast surface per bone surface; *BFR*, bone formation rate. *G–I*, bone marrow cells were cultured under four different conditions (*G*). *H* and *I*, number of TRAP$^+$ multinucleated cells (*MNCs*) on day 6 (*H*) and representative TRAP staining (*I*) of the cells in *G*; *, $p < 0.05$ ($n = 4$). *J*, TRAP$^+$ multinucleated cells in cultures of MDMs treated for 3 days with the indicated proteins (1 μg/ml) in the presence of 50 ng of RANKL/ml; *, $p < 0.05$ ($n = 4$). *K*, cell death during the osteoclastogenesis of MDMs treated with 60 ng of RANKL/ml plus 400 ng of netrin 1/ml, determined using an ELISA measuring the concentration of histone-DNA fragments in the culture supernatant ($n = 3$). *OD*, optical density. *L*, TRAP activity (measured in a TRAP solution assay) of MDMs cultured for 3 days in the presence of 50 ng of RANKL/ml plus 400 ng of netrin 1/ml ($n = 3$). *M* and *N*, MDMs plated on dentine slices and stimulated for 4 days with 100 ng of RANKL/ml plus 400 ng of netrin 1/ml. *M*, representative resorption pits (analyzed by scanning electron microscopy). *N*, multinucleated cell numbers, pit numbers, osteoclast area (*OC area*), and resorption pit area were quantified ($n = 4$).

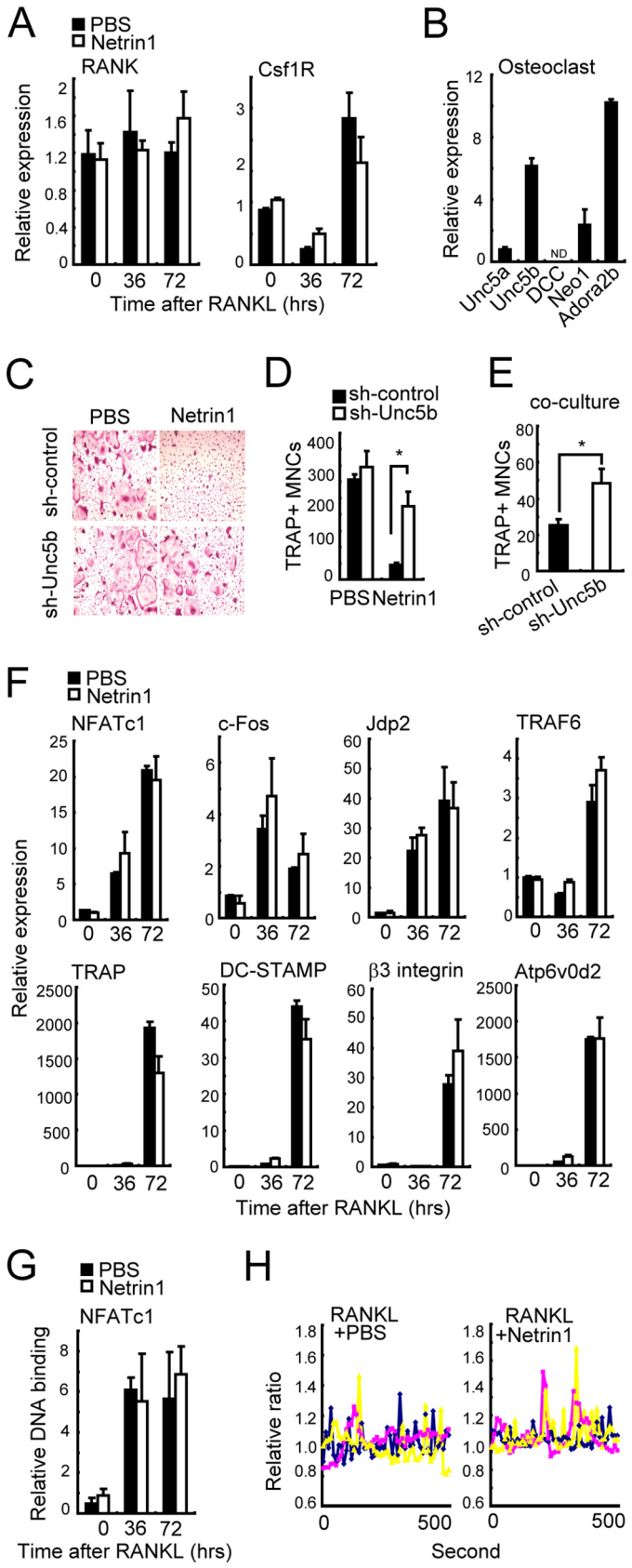

FIGURE 5. **Netrin 1 does not alter osteoclast differentiation.** *A*, RANK and Csf1R mRNA levels in MDMs stimulated with netrin 1 plus RANKL ($n = 3$). *B*, expression levels of netrin 1 receptors in osteoclasts ($n = 3$). *C* and *D*, representative TRAP staining (*C*), and osteoclast numbers (*D*) showing the effect of UNC5b knockdown (*sh-Unc5b*) on netrin 1-mediated osteoclast inhibition; *, $p < 0.05$ ($n = 4$). *E*, effect of UNC5b knockdown on the osteoclastogenesis of MDMs co-cultured with calvarial osteoblasts; *, $p < 0.05$ ($n = 4$). *F*, expression levels of osteoclast differentiation regulators in MDMs stimulated with netrin 1 plus RANKL ($n = 3$). *G*, DNA binding of NFATc1 in netrin 1-treated osteoclasts. *Error bars*, S.E. ($n = 3$). *H*, calcium imaging of MDMs treated with RANKL and netrin 1. Three representative traces of the changes in the fura-2 fluorescence ratio in the cells are shown.

the amount of bone erosion (Fig. 7*D*). The histological scores for inflammation in the hind paw were similar in netrin 1-treated and PBS-treated mice, but there were significantly fewer osteoclasts in the former (Fig. 7*E*). Finally, bone destruction was evaluated in a mouse model of CAIA using adult mice heterozygous for netrin 1 (Fig. 7, *G–J*). The clinical scores of netrin 1 heterozygous mice were normal (Fig. 7*H*), but the amount of bone erosion size was significantly higher than in the controls (Fig. 7, *I* and *J*). Although the histological scores for hind paw inflammation in the netrin 1 heterozygous mice were also normal, the number of osteoclasts in the calcaneus was increased (Fig. 7*J*). These data clearly demonstrated that netrin 1 protected the mice against autoimmune bone destruction *in vivo*.

Netrin 1 Increases Bone Mass—Age-related decreases in the serum netrin 1 concentration of the mice were determined (Fig. 8*A*). Netrin 1 expression was impaired in the bone marrow cells and mesenchymal stem cell (MSC)-derived osteoblasts of older *versus* younger mice (Fig. 8*B*). To gain insight into the mechanism underlying the age-dependent down-regulation of netrin 1, we measured the expression level of p53, a critical positive inducer of netrin 1 transcription (31), in the MSC-derived osteoblasts from mice of various ages. Both the expression and the binding of p53 to the netrin 1 promoter were impaired in MSC-derived osteoblasts from older *versus* younger mice (Fig. 8, *C* and *D*). Notably, netrin 1 was significantly lower in p53 knockdown osteoblasts (Fig. 8*E*), suggesting that abnormal p53 expression causes a decrease in netrin 1 expression in older mice.

To determine the impact of exogenous netrin 1 on the physiological condition of bone metabolism, 4-week-old (Fig. 8*F*) and 20-week-old (Fig. 8*L*) mice were intravenously injected with netrin 1 or PBS. Micro-computed tomography (μCT) and histological analysis of these mice showed an increase in bone volume (Fig. 8, *G*, *H*, *M*, and *N*). In addition, histomorphometric analysis revealed significant reductions in osteoclast parameters and increase in bone formation parameters (Fig, 8, *I*, *J*, and *O*). The normal expression of TRAP in the bone marrow cells of netrin 1-treated mice was also confirmed, whereas BMP-2 expression was increased (Fig. 8*K*). These findings suggest that netrin 1 induces BMP-2 and stimulates bone formation *in vivo*.

Discussion

Accumulating evidence suggests that the proinflammatory cytokines such as IL-17 and TNF-α are also potent stimulators of osteoclastogenesis. Although the contribution of osteoblasts and synovial fibroblasts to the pathogenesis of inflammatory bone destruction has been extensively characterized, bone-protective factors produced from these cells during inflammation have been largely overlooked. In this study, we identified netrin 1 as an osteoblast- or synovial fibroblast-derived soluble pro-

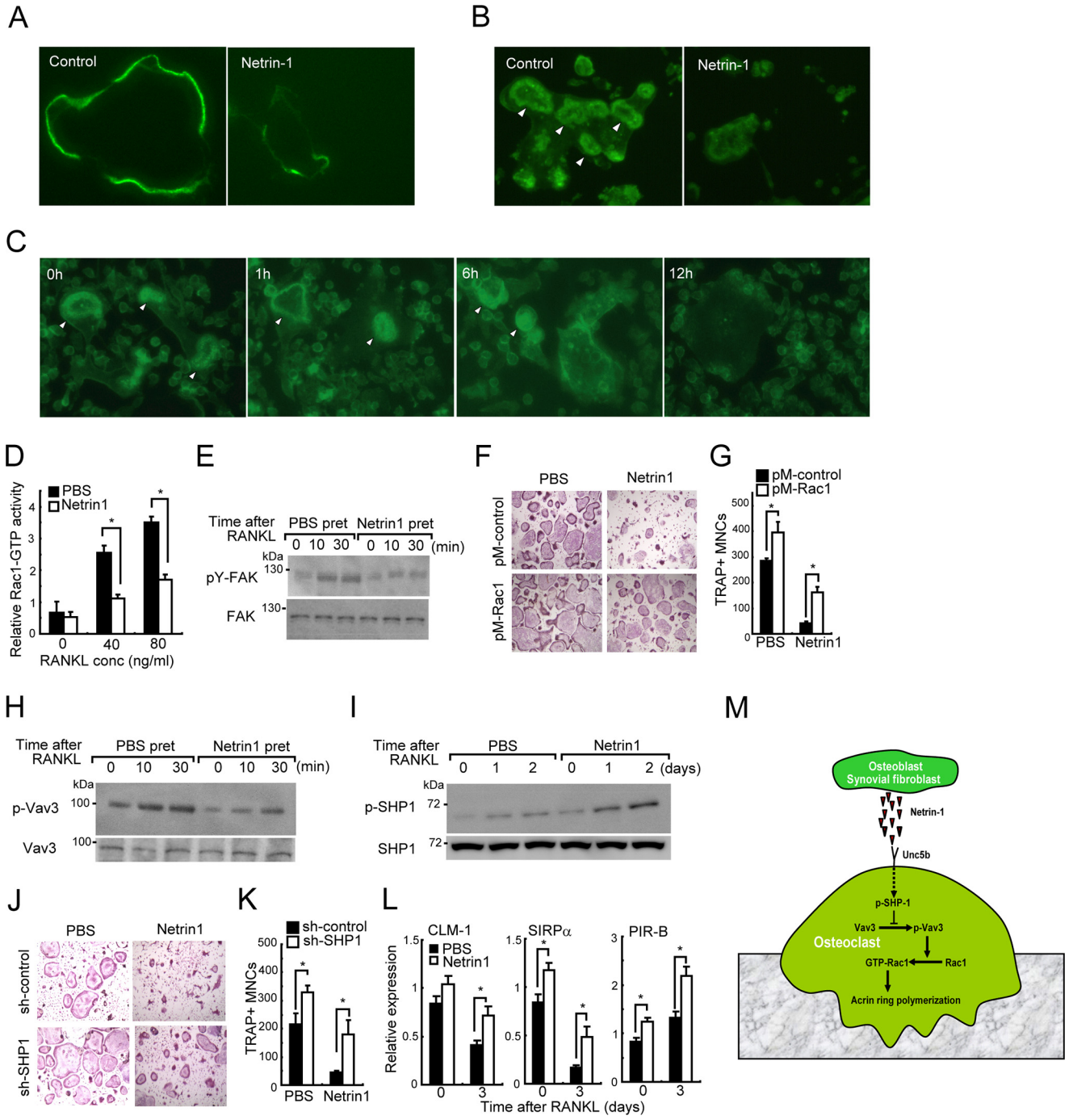

FIGURE 6. **Netrin 1 inhibits VAV3-RAC1 signaling.** *A* and *B*, representative images of the actin belt (*A*, *arrowheads*) and actin ring (*B*, *arrowheads*) in netrin 1-treated osteoclasts stained for F-actin using phalloidin. MDMs were stimulated with 50 ng/ml RANKL plus 400 ng/ml netrin 1 for 3 days on culture plates (*A*) or dentine slices (*B*). *C*, matured osteoclasts were stimulated by 400 ng/ml netrin 1 for 1, 6, or 12 h on dentine slices. Representative images of actin rings (*arrowheads*) in phalloidin-stained netrin 1-treated osteoclasts are shown. *D*, GTP-bound active RAC1 levels in netrin 1-treated osteoclasts; *, $p < 0.05$ ($n = 3$). *E*, MDMs treated with netrin 1 for 24 h and then stimulated with RANKL for the indicated times. Cell lysates were subjected to immunoblotting analysis with anti-Tyr(P)-FAK (*anti-pY-FAK*) and anti-FAK antibodies. *pret*, pretreatment. *F* and *G*, effect of constitutively active RAC1 (pM-RAC1) on the osteoclastogenesis of MDMs stimulated with RANKL plus netrin 1. Representative TRAP staining is shown in *F*, and osteoclast numbers were counted in *G*; *, $p < 0.05$ ($n = 4$). *H*, Vav3 phosphorylation in MDMs treated with netrin 1 for 24 h and then stimulated with RANKL for the indicated times. *I*, SHP-1 phosphorylation in MDMs treated with netrin 1 plus RANKL for the indicated number of days. *J* and *K*, TRAP staining (*J*) and osteoclast numbers (*K*) showing the effect of SHP1 knockdown on the osteoclastogenesis of MDMs stimulated with RANKL and netrin 1; *, $p < 0.05$ ($n = 4$). *L*, qPCR analysis of CLM-1, SIRPα, and PIR-B in MDMs treated with netrin 1 for 24 h and then stimulated with RANKL. *Error bars*, S.E.; *, $p < 0.05$ ($n = 3$). *M*, model of the regulation of osteoclast fusion by netrin 1.

tein that limits osteoclast multinucleation. Among the netrin family proteins, only netrin 1 is strongly expressed by osteoblasts and synovial fibroblasts, and its expression is dramatically enhanced by IL-17. To our knowledge, our study is the first to highlight that osteoblasts and synovial fibroblasts rapidly release humoral factors that protect against excessive bone destruction during acute inflammation. Importantly, in the synovial fluid of OA patients, netrin 1 concentration correlated

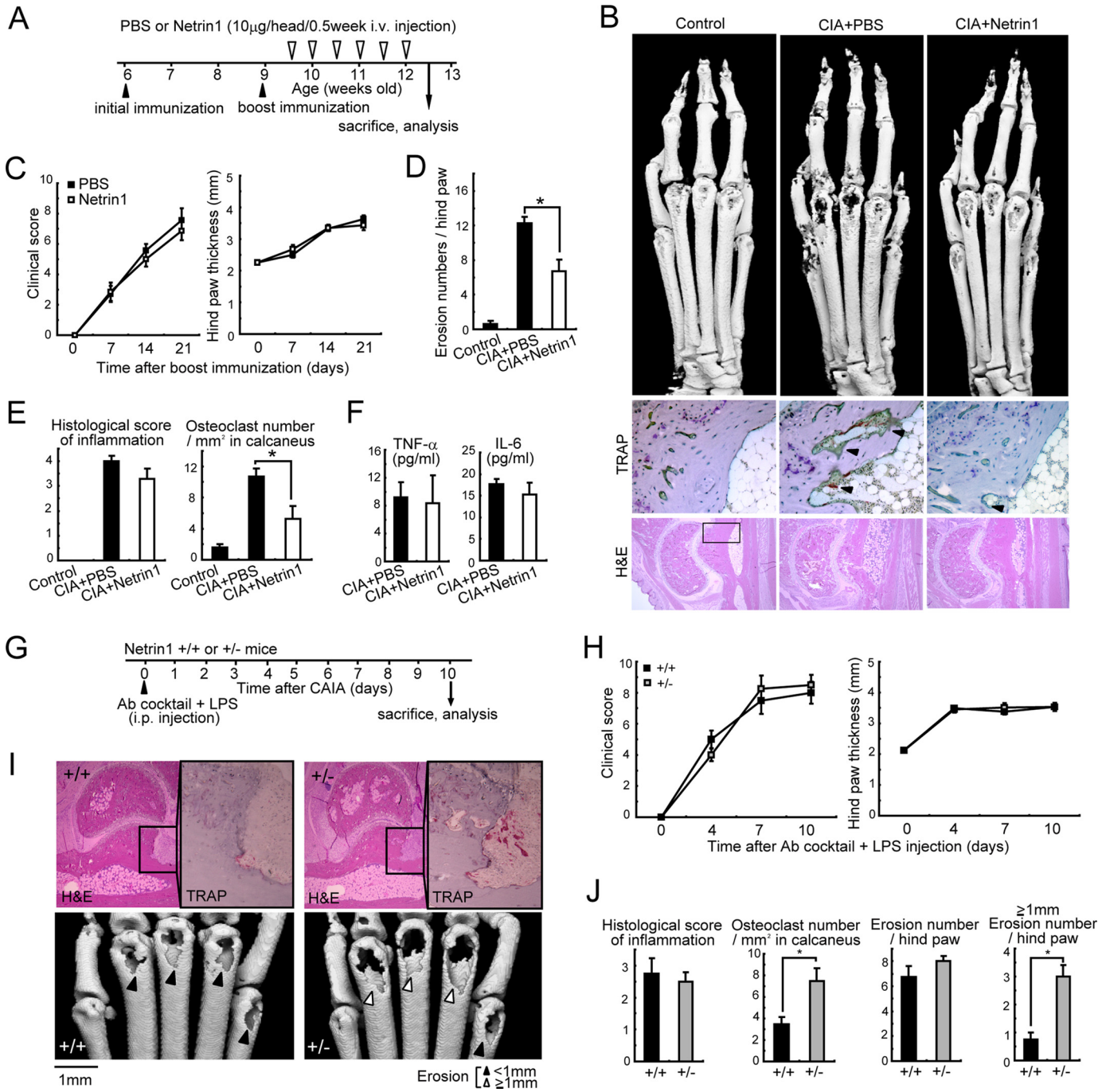

FIGURE 7. **Arthritic bone degradation was cured by Netrin 1.** *A–F*, protocol of CIA induction and netrin 1 administration in DBA/1J mice (*A*). *B*, representative histological and μCT images of the hind paw. *Top*, μCT images; *middle*, TRAP staining of the calcaneus; *bottom*, H&E staining of the ankle joint. The *rectangle* in the bottom image indicates the area shown in the middle image; the *arrowheads* indicate osteoclasts. *C* and *D*, clinical arthritis score and hind paw thickness (*C*) and degree of erosion in the hind paw (*D*). *E*, histological scores of the ankle joints and calcaneal osteoclast numbers. *F*, serum proinflammatory cytokines determined using ELISAs; *, $p < 0.05$ ($n = 5–7$). *G–J*, protocol of CAIA induction in 11-week-old wild-type mice and mice heterozygous for netrin 1 (*G*). *Ab cocktail*, antibody cocktail. *H*, clinical arthritis score and hind paw thickness . I, representative H&E staining, TRAP staining, and μCT images of the hind paws in the two groups of mice. *Top*, H&E and TRAP staining of the ankle joints; *bottom*, μCT images of the hind paw; *filled arrowheads*, major axis length of erosion <1 mm; *open arrowheads*, major axis length of erosion ≥1 mm. *J*, histological scores of the ankle joints, calcaneal osteoclast numbers, and hind paw erosion numbers. *Error bars*, S.E.; *, $p < 0.05$ ($n = 4$).

negatively with that of CTXI. This observation indicates that netrin 1 may also be a negative regulator of bone destruction in non-inflammatory conditions. Furthermore, netrin 1 treatment potently suppressed the bone erosion associated with experimental arthritis in mice, suggesting the prophylactic potential of netrin 1 in Th17-associated bone disease in humans. In this study, we also found that the osteoclast inhibitory function of netrin 1 is the strongest among the axon guidance cues released from osteoblasts. Previous studies showed 50% inhibition of osteoclast differentiation by 2 μg of "clustered" EphB4/ml (25) and 1 μg of Sema3A/ml, although when Sema3A is added after RANKL treatment, the inhibitory effect

is not observed (24, 32). By contrast, our results showed that 1 μg of netrin 1/ml inhibited osteoclast multinucleation by >95%, even when it was added after RANKL treatment. Netrin 1 is a member of the laminin-related family of matrix-binding proteins, which contain domain VI, three EGF-like repeats, and a heparin-binding domain. Therefore, netrin 1 most likely binds the extracellular matrix, which in turn regulates its local concentration and tissue bioavailability. Consequently, the local concentration of netrin 1 is likely to be very high around osteoblasts and synovial cells, both of which secrete various

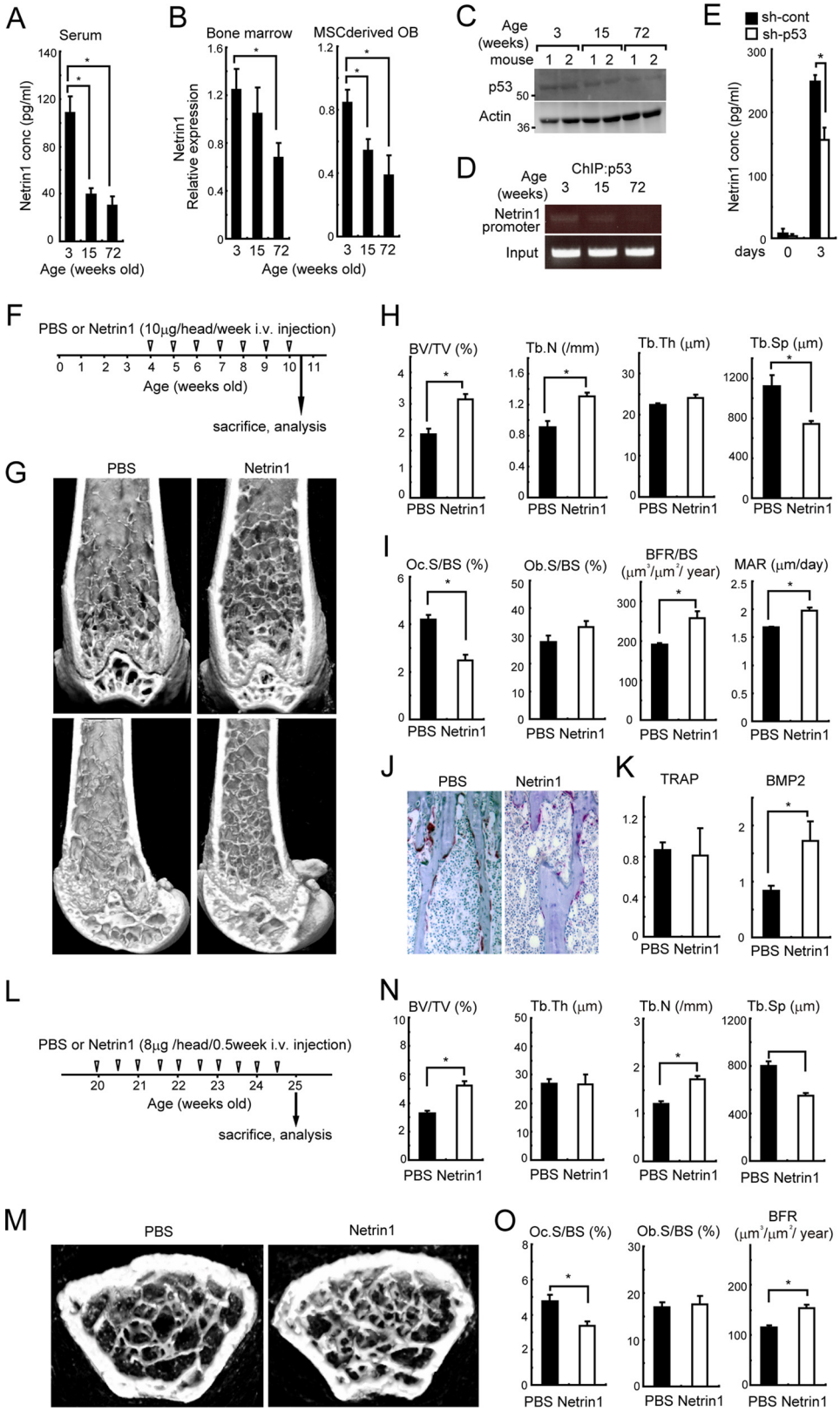

extracellular matrix components. Nevertheless, further investigation is needed to understand the *in vivo* bioavailability of netrin 1.

Our study is also the first to show that netrin 1 is a strong inhibitor of osteoclast fusion. The netrin 1 receptor UNC5b is potently expressed in osteoclasts. Netrin 1 binding to UNC5b causes the activation of SHP1, which, by suppressing VAV3 and RAC1 activation, leads to impaired osteoclast fusion. SHP1 is a phosphatase, and a reduction in its activity increases osteoclast multinucleation (33). In netrin 1-treated osteoclasts, the expression of ITIM-harboring receptors such as PIR-B and SIRPα was increased. Because this group of receptors activates SHP-1, it may be a target of UNC5b signaling. Further studies are required to understand the mechanism by which netrin 1 inhibits osteoclast fusion, but our data clearly indicate that VAV3-RAC1 signaling is inhibited by the netrin 1-UNC5b axis.

A recent study showed that netrin 1 is expressed in murine osteoclasts and stimulates their differentiation in an autocrine fashion (34). However, when we compared these results with osteoblasts and synovial fibroblasts, we found that netrin 1 is barely expressed in osteoclasts at both the mRNA and the protein levels. Significantly, osteoblasts and synovial fibroblasts exhibited more than 200-fold higher expression of netrin 1. Importantly, this comparison of netrin 1 expression between different cell types has not been done previously. Thus, we believe that the major source of netrin 1 inhibiting multinucleation of osteoclasts derives from osteoblasts. A previous study also showed enhanced *in vitro* osteoclastogenesis in netrin 1 knockdown osteoclasts (34). The lack of netrin 1 in osteoclasts may affect the signaling that regulates the intracellular differentiation of these cells (34). However, no enhancement of RANKL-induced osteoclastogenesis by netrin 1 knockdown in MDMs was observed in our experiment (data not shown). Strikingly, these previous studies also showed that 250 ng/ml recombinant netrin 1 (R&D Systems) significantly enhances (1.2-fold) the RANKL-induced osteoclast numbers. Discrepancies between our findings and their study may be explained by the differences between culture conditions. To generate osteoclasts, they changed media every 3 days, and after 7 days, they analyzed the number of osteoclasts. We did not change the culture media and performed analysis at days 3–5. Under our protocol, most of the osteoclasts underwent apoptosis at day 6. Because netrin 1 injection has a bone-protective function *in vivo*, we believe that the *in vitro* culture methods in Ref. 34 do not reflect the *in vivo* prophylactic potential of netrin 1. A previous study also showed a slight increase in the bone volume of wild-type mice engrafted with netrin 1 knock-out fetal liver cells (34). Because netrin 1 mediates adhesion of immune cells and promotes chemotaxis of CXCL12 (35), such results may reflect the difference of the stem cell trafficking to the bone marrow cavity. Generation of osteoclast/osteoblast-specific conditional netrin 1 knock-out mice will contribute to clarifying the role of netrin 1 in osteoclasts.

Previous work also suggested that the administration of netrin 1 inhibits inflammation in several models of animal disease (36, 37), but in our CIA mice, an anti-inflammatory effect of netrin 1 was not detected. Indeed, netrin 1 may not always exhibit anti-inflammatory activity, and contradictory results have been reported. For instance, plasma IL-6 levels were 50% lower in netrin 1 transgenic mice than in wild-type mice (38). Another study (39) demonstrated that although interference with netrin 1 levels does not affect inflammation, it does prevent tumor progression in a mouse model of inflammatory bowel disease-associated colorectal cancer. However, in two studies, netrin 1 promoted atherosclerosis and inflammation by inhibiting macrophage movement (40, 41). In our models of bone destruction (CIA and CAIA), netrin 1 did not significantly modulate inflammation. Thus, our data collectively suggest that netrin 1 does not modulate arthritic inflammation; rather, it may modulate inflammation only under certain conditions, but not in the context of bone-destructive diseases. The potential anti-inflammatory function of netrin 1 remains to be evaluated in further experiments.

We also found that serum netrin 1 concentrations decline during aging and that the administration of netrin 1 to healthy mice inhibited osteoclast fusion, thus increasing their bone volume. Although netrin 1 had no effect on osteoblastogenesis *in vitro*, it increased the bone formation rate *in vivo*. Bone remodeling in DC-STAMP (10) and ATP6v0d2 (9) gene knock-out mice is uncoupled, as osteoclast parameters are reduced, whereas bone formation rates are increased. In cells from these mice, *in vitro* osteoclast fusion was significantly impaired, whereas *in vitro* osteoblastogenesis was normal, suggesting that the former stimulates bone formation *in vivo*. Our *in vitro* study indicated that netrin 1 released by osteoblasts induces the CREB-dependent expression of BMP-2 from osteoclasts, which stimulates osteoblastogenesis. This mechanism was confirmed *in vivo*, because BMP-2 expression was increased in the femurs of netrin 1-injected mice. According to these findings, the administration of netrin 1 stimulates bone formation via osteoclast-derived BMP-2. These observations demonstrate the potential of netrin 1 as a prophylactic agent in osteoporosis and in a broad range of other bone-destructive diseases.

Although to date, studies of netrin 1 have focused on its neurobiological role, our results clearly show that netrin 1 suppresses osteoclast fusion, both *in vivo* and *in vitro*. Further studies of netrin 1, including netrin 1-UNC5b signaling in osteoclasts, together with the generation of conditional netrin 1

FIGURE 8. **Bone protection by Netrin 1.** *A*, serum netrin 1 concentrations in mice of different ages as measured using an ELISA; *, $p < 0.05$ ($n = 3$). *B*, qPCR analysis of netrin 1 expression in the bone marrow cells and mesenchymal stem cell-derived osteoblasts (*OB*) from mice of different ages; *, $p < 0.05$ ($n = 4$). *C–E*, the expression of p53 in mesenchymal stem cell-derived osteoblasts from mice of different ages (*C*, $n = 2$/age). *D*, ChIP analysis of the lysates from the cells in *C* using a p53 antibody. *E*, effect of p53 knockdown on netrin 1 production by osteoblasts ; *, $p < 0.05$ ($n = 3$). *F–K*, protocol of netrin 1 administration to young C57BL/6 mice (*F*). *G* and *H*, the distal femur was visualized (*G*, *top*, coronal images; *bottom*, sagittal images) and analyzed by μCT (*H*). *BV/TV*, bone volume per tissue volume; *Tb.N*, trabecular bone number; *Tb.Th*, trabecular bone thickness; *Tb.Sp*, trabecular bone spacing. *I* and *J*, bone histomorphometric analysis (*I*) and TRAP staining (*J*) of the metaphyseal portion of the tibia. *K*, mRNA levels of TRAP and BMP2 in bone marrow cells. *Oc.S/BS*, osteoclast surface per bone surface; *Ob.S/BS*, osteoblast surface per bone surface; *MAR*, mineral apposition rate; *BFR*, bone formation rate. *Error bars*, S.E.; *, $p < 0.05$ ($n = 4–5$). *L–O*, protocol of netrin 1 administration in old C57BL/6 mice (*L*). *M*, representative μCT images of distal femurs. *N* and *O*, bone morphometric analysis (*N*) and bone histomorphometric analysis of the metaphyseal portion of the tibia (*O*); *, $p < 0.05$ ($n = 3–4$).

gene knock-out mice, will contribute to clarifying the role of netrin 1 in bone metabolism.

Experimental Procedures

Mice—Female C57BL/6 mice and female DBA/1J mice were purchased from CLEA Japan and Japan SLC, respectively. ICR or C57BL/6 background female mice heterozygous for a netrin 1 mutation (16) were crossed to obtain homozygous embryos. All animal experiments were performed with the approval of the Animal Research Committee of the Research Institute for Microbial Diseases, Osaka University.

Cells and Reagents—Synovial fibroblasts were harvested as described previously (42). Briefly, the articular capsules of the ankle joints isolated from the hind paw of mice with CIA were treated with 1 mg of collagenase/ml. The resulting suspension was filtered through a 40-μm cell strainer. The filtered cells were cultured in DMEM supplemented with 10% FCS and 50 mg of L-glutamine/ml for 24 h and then washed with PBS. Adherent cells from passage 3 were used as synovial fibroblasts. B cells and T cells were collected from the spleen by positive selection using anti-B220 and anti-Thy-1.2 magnetic beads (Miltenyi Biotec, Bergisch Gladbach, Germany), respectively. Splenic $CD11b^+$ macrophages were sorted using a FACSAria flow cytometer (BD Biosciences). Dendritic cells were isolated by positive selection using anti-CD11c magnetic beads (Miltenyi Biotec). Th1, Th2, and Th17 cells were generated from $CD4^+$ cells isolated from splenocytes using anti-CD4 magnetic beads (Miltenyi Biotec), as described previously (43). Recombinant murine M-CSF, IL-17A, IL-4, IL-6, IL-12, and IFN-γ were purchased from PeproTech. Recombinant RANKL, netrin 1, netrin 4, Sema3A-Fc, and EphB4-Fc were purchased from R&D Systems. TNF and IL-6 ELISA kits were purchased from R&D Systems. ELISA kits were used for analyses of mouse CTXI (USCN Life Science), human CTXI (MBS454442, MyBioSource), mouse netrin 1 (E91827Mu (USCN Life Science), human netrin 1 (E91827Hu, USCN Life Science), human IL-17A (Diaclone SAS), and human IFN-γ (KHC4021, Invitrogen). The ALP quantification kit (LabAssay) was purchased from Wako (Tokyo, Japan). Nuclear extracts were prepared as described (44). The DNA binding activities of NFATc1 was quantified using a TransAM transcription factor assay (Active Motif, Carlsbad, CA). The histone-DNA fragment in the culture supernatant was quantified using a cell death detection ELISA (Roche Applied Science). The NF-κB inhibitor BAY117085 was from R&D Systems. OM was prepared from MDMs cultured with 40 ng of netrin 1/ml and/or 100 ng of RANKL/ml for 4 days, after which the culture medium was concentrated 10-fold using an Amicon Centricon Plus-70 concentrator. Antibodies for FACS analysis were from BD Biosciences. Data were collected using a FACSCalibur (BD Biosciences) and analyzed by FlowJo (Ashland, OR).

Osteoclast/Osteoblast Culture—MDMs were prepared as described (45). Osteoclasts were generated by incubating the cells with 25 ng of M-CSF/ml and various concentrations of RANKL. TRAP staining was performed as described (46). For the pit assay, MDMs were plated on dentine slices with RANKL. After 5 days, the cells were immersed for 3 h in 1 M NH_4OH, after which pit numbers were counted. Calvariae from 2-day-old mice were collected as described previously (46). Mesenchymal stem cells from compact bone were prepared as described previously (47). Osteoblastogenesis was induced by culturing the cells with an osteoblast-inducing reagent (Takara). ALP and calcified nodules were stained using TRAP/ALP (Wako) and calcified nodule (AK-21; Primary Cell Co. Ltd., Hokkaido, Japan) staining kits, respectively. The calcium concentration was quantified using the Metallo Assay LS-MPR kit (AKJ Global Technology). For osteoclast/osteoblast co-culture, MDMs (6×10^5) and calvarial cells (5×10^5) were cultured in 24-well plates containing α-minimum essential medium supplemented with 30 nM $1\alpha,25(OH)_2D_3$ plus prostaglandin E_2 (PGE_2).

Immunoblotting and Chromatin Immunoprecipitation Assay—Western blotting was performed as described previously (44). Proteins were detected using anti-UNC5b (ABC89, Millipore), anti-p-VAV3 (ab109544, Abcam), anti-VAV3 (ab52938, Abcam), anti-p-FAK (3284, Cell Signaling), anti-FAK (3285, Cell Signaling), anti-p-SHP1 (D11G5, Abcam), anti-SHP1 (3759, Abcam), anti-p53 (sc-126, Santa Cruz Biotechnology), and anti-actin (C-11, Santa Cruz Biotechnology) antibodies. Chromatin was immunoprecipitated as described previously (11). Briefly, chromatin was precipitated in fixed cells using anti-CREB (48H2, Cell Signaling) and anti-p53 (sc-126, Santa Cruz Biotechnology) antibodies. The precipitated DNA was analyzed by PCR using primers able to detect BMP-2 and netrin 1 promoted sequences: 5′-GGCATCGCCCACGATGGCTG-3′ and 5′-CAAGTTCAAGAAGTCTCC-3′ and 5′-AACGCGGACTTTCCG-3′ and 5′-GAGAAGCTCTGCTTCC-3′, respectively (27–31).

Intracellular Calcium Imaging—MDMs were loaded for 30 min with 5 μM fura-2/AM in loading solution (115 mM NaCl, 5.4 mM KCl, 1 mM $MgCl_2$, 2 mM $CaCl_2$, 20 mM Hepes, 10 mM glucose, pH 7.42). Fluorescent activity was quantified as described previously (48).

PCR Analysis—RNA was extracted using TRIzol Reagent (Invitrogen Life Science Technologies). cDNA was generated using ReverTra Ace (Toyobo Co., Ltd, Japan). qPCR was performed with an ABI PRISM 7500 Real-Time PCR System using TaqMan Assays-on-Demand primers (NFATc1 (Mm00479445_m1); Jdp2 (Mm00473044_m1); c-Fos (Mm00487425_m1); Sema3a (Mm00436469_m1); Ephb4 (Mm01201157_m1); ALP (Mm01200300_m1); RUNX2 (Mm00501584_m1); RANK (Mm00437132_m1); UNC5a (Mm00462368_m1); UNC5b (Mm00504054_m1); DCC (Mm00514509_m1); Neo1 (Mm00476326_m1); Adora2b (Mm00839292_m1); BMP-2 (Mm01340178_m1); Csf1R (Mm01266652_m1); TRAF6 (Mm00493836_m1); TRAP (Mm00446003_m1); DC-STAMP (Mm01168058_m1); β3 integrin (Mm00443980_m1); ATP6v0d2 (Mm01222963_m1); CLM1 (Mm00441004_m1); SIRP-α(Mm00455928_m1); PIR-B (Mm01700366_m1); netrin 1 (Mm00500896_m1); Netrin 3 (Mm00477916_m1); Netrin 4 (Mm00480462_m1); NetrinG1 (Mm00453144_m1); NetrinG2 (Mm01325566_m1); RANKL (Mm00441906_m1); OPG (Mm00435454_m1); BMP2 (Mm01340178_m1); BMP6 (Mm01332882_m1); Sema4d (Mm00443147_m1); Sphk-1 (Mm00448841_g1); Wnt10b (Mm00442104_m1); HGF (Mm01135184_m1); PDGFB (Mm00440677_m1); LIF

(Mm00434762_g1); CTF-1 (Mm00432772_m1); and CXCL16 (Mm00469712_m1) Applied Biosystems, Foster City, CA). The quantity of mRNA was normalized to 18S rRNA using the Taq-Man ribosomal control reagent kit (Applied Biosystems).

Viral Gene Transfer/Knockdown—Retroviral constructs for constitutively active RAC1 (pM-RAC1) (49) and the retroviral particles (50) were generated as described previously. Control virus particles were generated using the empty pMIEG3 plasmid. Cells were transfected with the retroviral gene as described elsewhere (51). The transfectants were resuspended in DME medium containing 10% FCS and supplemented with 25 ng of M-CSF/ml. The medium was refreshed after 3 days, and the cells were stimulated with 60 ng of RANKL/ml plus 25 ng of M-CSF/ml to induce osteoclastogenesis. shRNA lentivirus of netrin 1 (sc-42045-V), UNC5b (sc-61847-V), SHP1 (sc-29479-V), CREB (sc-35111), p53 (sc-29436), and control shRNA lentiviral particles (sc-108080) were purchased from Santa Cruz Biotechnology. For lentiviral gene transfer, the virus in 2 μg of Polybrene/ml was added to cells. After 10 h, the cells were washed and cultured for 30 h with 2 μg of puromycin/ml, and the puromycin-resistant cells were identified.

Analysis of the Bone Phenotype—The bone formation rate was quantified by double calcein labeling (25). The bones were fixed in 70% ethanol, and the hind paws and femurs were analyzed by three-dimensional μCT using a Scan-Xmate RB080SS110 (Comscan Techno Co., Ltd, Sagamihara, Japan) and the TRI/3D-Bon software (Ratoc System Engineering Co., Ltd, Tokyo, Japan). Bone microarchitectural parameters in the trabecular regions were quantified in an area 0.1–1.5 mm from the chondro-osseous junction. Bone histomorphometric analysis was carried out in tibias stained with Villanueva bone stain (Wako) and embedded in methyl methacrylate. Serial longitudinal sections (6-mm-thick) were prepared using a microtome (RM2255, Leica) and analyzed with a Histometry RT camera (System Supply Co., Ltd, Nagano, Japan). Hind paw sections were stained with TRAP or H&E. Histological scores were graded from 0 to 4 based on a previously described scoring system (52).

Induction of Arthritis—Bovine type II collagen and complete Freund's adjuvant were purchased from Chondrex. To induce CIA in DBA/1J mice, the mice were immunized according to the manufacturer's protocol, using an emulsion of these two ingredients. To induce CAIA, 1.5 mg of Arthrogen-CIA arthritogenic monoclonal antibody (53040, Chondrex) and 25 mg of LPS were injected intraperitoneally into DBA/1J mice. The mice were then observed daily for signs of joint inflammation and scored for clinical signs as described previously (53). Briefly, joint inflammation was scored from 0 to 4, with 4 being the maximum arthritis score per paw, and 16 being the maximum score per mouse.

Synovial Fluid Collection—Synovial fluids from RA and OA patients (diagnosed according to the criteria for RA and OA of the American College of Rheumatology) were collected and analyzed by ELISA. All patients were >18 years of age. The inclusion criteria for patients with OA were the presence of osteophytes and joint space narrowing on an X-ray of Kellgren-Lawrence grade ≥2. For RA patients, they were: fulfillment of the 2010 American College of Rheumatology (ACR)/European League Against Rheumatism (EULAR) criteria for RA or the 1987 ACR criteria for RA. Juveniles were excluded from the study. The mean (±S.E.) ages of the OA and RA patients were 75.1 ± 6.1 and 65 ± 12.8 years, respectively. The experiments were performed with the approval of the Ethics Committee of the Kyoto University Graduate School of Medicine.

Statistical Analysis—Student's *t* test was used to evaluate the significance of the differences, indicated by a p level < 0.05.

Author Contributions—K. M. initiated, designed, and conducted the whole project. Takahiko Kawasaki provided netrin 1 knockout mice. M. Hamaguchi, M. Hashimoto, M. Furu, H. I., and T. F. provided synovial fluids from RA and OA patients. N. T, T. Karuppuchamy, T. Kondo, Takumi Kawasaki, M. Fukasaka, T. M., T. S., Y. S., M. M. M., and Y. K. contributed to the experiments. K. M. wrote the manuscript. S. A. supervised the overall research.

Acknowledgments—We thank Dr. X. R. Bustelo for providing the constitutively active RAC1 retrovirus plasmid (pM-RAC1), C. Coban for fruitful discussions, and E. Kamada and M. Kageyama for secretarial assistance.

References

1. Schett, G., and Gravallese, E. (2012) Bone erosion in rheumatoid arthritis: mechanisms, diagnosis and treatment. *Nat. Rev. Rheumatol.* **8,** 656–664
2. Karsenty, G., and Wagner, E. F. (2002) Reaching a genetic and molecular understanding of skeletal development. *Dev. Cell* **2,** 389–406
3. Takayanagi, H., Kim, S., Koga, T., Nishina, H., Isshiki, M., Yoshida, H., Saiura, A., Isobe, M., Yokochi, T., Inoue, J., Wagner, E. F., Mak, T. W., Kodama, T., and Taniguchi, T. (2002) Induction and activation of the transcription factor NFATc1 (NFAT2) integrate RANKL signaling in terminal differentiation of osteoclasts. *Dev. Cell* **3,** 889–901
4. Kawaida, R., Ohtsuka, T., Okutsu, J., Takahashi, T., Kadono, Y., Oda, H., Hikita, A., Nakamura, K., Tanaka, S., and Furukawa, H. (2003) Jun dimerization protein 2 (JDP2), a member of the AP-1 family of transcription factor, mediates osteoclast differentiation induced by RANKL. *J. Exp. Med.* **197,** 1029–1035
5. Maruyama, K., Fukasaka, M., Vandenbon, A., Saitoh, T., Kawasaki, T., Kondo, T., Yokoyama, K. K., Kidoya, H., Takakura, N., Standley, D., Takeuchi, O., and Akira, S. (2012) The transcription factor Jdp2 controls bone homeostasis and antibacterial immunity by regulating osteoclast and neutrophil differentiation. *Immunity* **37,** 1024–1036
6. Grigoriadis, A. E., Wang, Z. Q., Cecchini, M. G., Hofstetter, W., Felix, R., Fleisch, H. A., and Wagner, E. F. (1994) c-Fos: a key regulator of osteoclast-macrophage lineage determination and bone remodeling. *Science* **266,** 443–448
7. Franzoso, G., Carlson, L., Xing, L., Poljak, L., Shores, E. W., Brown, K. D., Leonardi, A., Tran, T., Boyce, B. F., and Siebenlist, U. (1997) Requirement for NF-κB in osteoclast and B-cell development. *Genes Dev.* **11,** 3482–3496
8. Okamoto, K., and Takayanagi, H. (2011) Regulation of bone by the adaptive immune system in arthritis. *Arthritis Res. Ther.* **13,** 219
9. Lee, S. H., Rho, J., Jeong, D., Sul, J. Y., Kim, T., Kim, N., Kang, J. S., Miyamoto, T., Suda, T., Lee, S. K., Pignolo, R. J., Koczon-Jaremko, B., Lorenzo, J., and Choi, Y. (2006) v-ATPase V_0 subunit d2-deficient mice exhibit impaired osteoclast fusion and increased bone formation. *Nat. Med.* **12,** 1403–1409
10. Yagi, M., Miyamoto, T., Sawatani, Y., Iwamoto, K., Hosogane, N., Fujita, N., Morita, K., Ninomiya, K., Suzuki, T., Miyamoto, K., Oike, Y., Takeya, M., Toyama, Y., and Suda, T. (2005) DC-STAMP is essential for cell-cell fusion in osteoclasts and foreign body giant cells. *J. Exp. Med.* **202,** 345–351
11. Maruyama, K., Uematsu, S., Kondo, T., Takeuchi, O., Martino, M. M., Kawasaki, T., and Akira, S. (2013) Strawberry notch homologue 2 regu-

lates osteoclast fusion by enhancing the expression of DC-STAMP. *J. Exp. Med.* **210,** 1947–1960
12. Cohen, S. B., Dore, R. K., Lane, N. E., Ory, P. A., Peterfy, C. G., Sharp, J. T., van der Heijde, D., Zhou, L., Tsuji, W., Newmark, R., and Denosumab Rheumatoid Arthritis Study Group (2008) Denosumab treatment effects on structural damage, bone mineral density, and bone turnover in rheumatoid arthritis: a twelve-month, multicenter, randomized, double-blind, placebo-controlled, phase II clinical trial. *Arthritis Rheum.* **58,** 1299–1309
13. Rachner, T. D., Khosla, S., and Hofbauer, L. C. (2011) Osteoporosis: now and the future. *Lancet* **377,** 1276–1287
14. Reginster, J. Y., Pelousse, F., and Bruyère, O. (2013) Safety concerns with the long-term management of osteoporosis. *Expert Opin. Drug Saf.* **12,** 507–522
15. Teitelbaum, S. L. (2011) The osteoclast and its unique cytoskeleton. *Ann. N.Y. Acad. Sci.* **1240,** 14–17
16. Serafini, T., Colamarino, S. A., Leonardo, E. D., Wang, H., Beddington, R., Skarnes, W. C., and Tessier-Lavigne, M. (1996) Netrin-1 is required for commissural axon guidance in the developing vertebrate nervous system. *Cell* **87,** 1001–1014
17. Kennedy, T. E., Serafini, T., de la Torre, J. R., and Tessier-Lavigne, M. (1994) Netrins are diffusible chemotropic factors for commissural axons in the embryonic spinal cord. *Cell* **78,** 425–435
18. Colamarino, S. A., and Tessier-Lavigne, M. (1995) The axonal chemoattractant netrin-1 is also a chemorepellent for trochlear motor axons. *Cell* **81,** 621–629
19. Lai Wing Sun, K., Correia, J. P., and Kennedy, T. E. (2011) Netrins: versatile extracellular cues with diverse functions. *Development* **138,** 2153–2169
20. Cirulli, V., and Yebra, M. (2007) Netrins: beyond the brain. *Nat. Rev. Mol. Cell Biol.* **8,** 296–306
21. van Gils, J. M., Derby, M. C., Fernandes, L. R., Ramkhelawon, B., Ray, T. D., Rayner, K. J., Parathath, S., Distel, E., Feig, J. L., Alvarez-Leite, J. I., Rayner, A. J., McDonald, T. O., O'Brien, K. D., Stuart, L. M., Fisher, E. A., *et al.* (2012) The neuroimmune guidance cue netrin-1 promotes atherosclerosis by inhibiting the emigration of macrophages from plaques. *Nat. Immunol.* **13,** 136–143
22. Ly, N. P., Komatsuzaki, K., Fraser, I. P., Tseng, A. A., Prodhan, P., Moore, K. J., and Kinane, T. B. (2005) Netrin-1 inhibits leukocyte migration *in vitro* and *in vivo*. *Proc. Natl. Acad. Sci. U.S.A.* **102,** 14729–14734
23. Togari, A., Mogi, M., Arai, M., Yamamoto, S., and Koshihara, Y. (2000) Expression of mRNA for axon guidance molecules, such as semaphorin-III, netrins and neurotrophins, in human osteoblasts and osteoclasts. *Brain Res.* **878,** 204–209
24. Hayashi, M., Nakashima, T., Taniguchi, M., Kodama, T., Kumanogoh, A., and Takayanagi, H. (2012) Osteoprotection by semaphorin 3A. *Nature* **485,** 69–74
25. Zhao, C., Irie, N., Takada, Y., Shimoda, K., Miyamoto, T., Nishiwaki, T., Suda, T., and Matsuo, K. (2006) Bidirectional ephrinB2-EphB4 signaling controls bone homeostasis. *Cell Metab.* **4,** 111–121
26. Enoki, Y., Sato, T., Tanaka, S., Iwata, T., Usui, M., Takeda, S., Kokabu, S., Matsumoto, M., Okubo, M., Nakashima, K., Yamato, M., Okano, T., Fukuda, T., Chida, D., Imai, Y., *et al.* (2014) Netrin-4 derived from murine vascular endothelial cells inhibits osteoclast differentiation *in vitro* and prevents bone loss *in vivo*. *FEBS Lett.* **588,** 2262–2269
27. Zhang, R., Edwards, J. R., Ko, S. Y., Dong, S., Liu, H., Oyajobi, B. O., Papasian, C., Deng, H. W., and Zhao, M. (2011) Transcriptional regulation of BMP2 expression by the PTH-CREB signaling pathway in osteoblasts. *PLoS ONE* **6,** e20780
28. Chung, D. H., Humphrey, M. B., Nakamura, M. C., Ginzinger, D. G., Seaman, W. E., and Daws, M. R. (2003) CMRF-35-like molecule-1, a novel mouse myeloid receptor, can inhibit osteoclast formation. *J. Immunol.* **171,** 6541–6548
29. van Beek, E. M., de Vries, T. J., Mulder, L., Schoenmaker, T., Hoeben, K. A., Matozaki, T., Langenbach, G. E., Kraal, G., Everts, V., and van den Berg, T. K. (2009) Inhibitory regulation of osteoclast bone resorption by signal regulatory protein α. *FASEB. J.* **23,** 4081–4090
30. Mori, Y., Tsuji, S., Inui, M., Sakamoto, Y., Endo, S., Ito, Y., Fujimura, S., Koga, T., Nakamura, A., Takayanagi, H., Itoi, E., and Takai, T. (2008) Inhibitory immunoglobulin-like receptors LILRB and PIR-B negatively regulate osteoclast development. *J. Immunol.* **181,** 4742–4751
31. Paradisi, A., Creveaux, M., Gibert, B., Devailly, G., Redoulez, E., Neves, D., Cleyssac, E., Treilleux, I., Klein, C., Niederfellner, G., Cassier, P. A., Bernet, A., and Mehlen, P. (2013) Combining chemotherapeutic agents and netrin-1 interference potentiates cancer cell death. *EMBO Mol. Med.* **5,** 1821–1834
32. Fukuda, T., Takeda, S., Xu, R., Ochi, H., Sunamura, S., Sato, T., Shibata, S., Yoshida, Y., Gu, Z., Kimura, A., Ma, C., Xu, C., Bando, W., Fujita, K., Shinomiya, K., *et al.* (2013) Sema3A regulates bone-mass accrual through sensory innervations. *Nature* **497,** 490–493
33. Aoki, K., Didomenico, E., Sims, N. A., Mukhopadhyay, K., Neff, L., Houghton, A., Amling, M., Levy, J. B., Horne, W. C., and Baron, R. (1999) The tyrosine phosphatase SHP-1 is a negative regulator of osteoclastogenesis and osteoclast resorbing activity: increased resorption and osteopenia in me^v/me^v mutant mice. *Bone* **25,** 261–267
34. Mediero, A., Ramkhelawon, B., Perez-Aso, M., Moore, K. J., and Cronstein, B. N. (2015) Netrin-1 is a critical autocrine/paracrine factor for osteoclast differentiation. *J. Bone Miner. Res.* **30,** 837–854
35. Guo, X. K., Liu, Y. F., Zhou, Y., Sun, X. Y., Qian, X. P., Zhang, Y., and Zhang, J. (2013) The expression of netrin-1 in the thymus and its effects on thymocyte adhesion and migration. *Clin. Dev. Immunol.* **2013,** 462152
36. Mirakaj, V., Gatidou, D., Pötzsch, C., König, K., and Rosenberger, P. (2011) Netrin-1 signaling dampens inflammatory peritonitis. *J. Immunol.* **186,** 549–555
37. Mirakaj, V., Dalli, J., Granja, T., Rosenberger, P., and Serhan, C. N. (2014) Vagus nerve controls resolution and pro-resolving mediators of inflammation. *J. Exp. Med.* **211,** 1037–1048
38. Ranganathan, P., Jayakumar, C., Santhakumar, M., and Ramesh, G. (2013) Netrin-1 regulates colon-kidney cross talk through suppression of IL-6 function in a mouse model of DSS-colitis. *Am. J. Physiol. Renal Physiol.* **304,** F1187–1197
39. Paradisi, A., Maisse, C., Coissieux, M. M., Gadot, N., Lépinasse, F., Delloye-Bourgeois, C., Delcros, J. G., Svrcek, M., Neufert, C., Fléjou, J. F., Scoazec, J. Y., and Mehlen, P. (2009) Netrin-1 up-regulation in inflammatory bowel diseases is required for colorectal cancer progression. *Proc. Natl. Acad. Sci. U.S.A.* **106,** 17146–17151
40. Ramkhelawon, B., Hennessy, E. J., Ménager, M., Ray, T. D., Sheedy, F. J., Hutchison, S., Wanschel, A., Oldebeken, S., Geoffrion, M., Spiro, W., Miller, G., McPherson, R., Rayner, K. J., and Moore, K. J. (2014) Netrin-1 promotes adipose tissue macrophage retention and insulin resistance in obesity. *Nat. Med.* **20,** 377–384
41. Gerszten, R. E., and Tager, A. M. (2012) The monocyte in atherosclerosis: Should I stay or should I go now? *N. Engl. J. Med.* **366,** 1734–1736
42. Gao, B., Calhoun, K., and Fang, D. (2006) The proinflammatory cytokines IL-1β and TNF-α induce the expression of Synoviolin, an E3 ubiquitin ligase, in mouse synovial fibroblasts via the Erk1/2-ETS1 pathway. *Arthritis Res. Ther.* **8,** R172
43. Sato, K., Suematsu, A., Okamoto, K., Yamaguchi, A., Morishita, Y., Kadono, Y., Tanaka, S., Kodama, T., Akira, S., Iwakura, Y., Cua, D. J., and Takayanagi, H. (2006) Th17 functions as an osteoclastogenic helper T cell subset that links T cell activation and bone destruction. *J. Exp. Med.* **203,** 2673–2682
44. Kawagoe, T., Takeuchi, O., Takabatake, Y., Kato, H., Isaka, Y., Tsujimura, T., and Akira, S. (2009) TANK is a negative regulator of Toll-like receptor signaling and is critical for the prevention of autoimmune nephritis. *Nat. Immunol.* **10,** 965–972
45. Maruyama, K., Takada, Y., Ray, N., Kishimoto, Y., Penninger, J. M., Yasuda, H., and Matsuo, K. (2006) Receptor activator of NF-κB ligand and osteoprotegerin regulate proinflammatory cytokine production in mice. *J. Immunol.* **177,** 3799–3805
46. Maruyama, K., Kawagoe, T., Kondo, T., Akira, S., and Takeuchi, O. (2012) TRAF family member-associated NF-κB activator (TANK) is a negative regulator of osteoclastogenesis and bone formation. *J. Biol. Chem.* **287,** 29114–29124
47. Zhu, H., Guo, Z. K., Jiang, X. X., Li, H., Wang, X. Y., Yao, H. Y., Zhang, Y., and Mao, N. (2010) A protocol for isolation and culture of mesenchymal stem cells from mouse compact bone. *Nat. Protoc.* **5,** 550–560

48. Kuroda, Y., Hisatsune, C., Nakamura, T., Matsuo, K., and Mikoshiba, K. (2008) Osteoblasts induce Ca^{2+} oscillation-independent NFATc1 activation during osteoclastogenesis. *Proc. Natl. Acad. Sci. U.S.A.* **105,** 8643–8648
49. Guo, F., and Zheng, Y. (2004) Rho family GTPases cooperate with *p53* deletion to promote primary mouse embryonic fibroblast cell invasion. *Oncogene* **23,** 5577–5585
50. Gonzalo, P., Guadamillas, M. C., Hernández-Riquer, M. V., Pollán, A., Grande-García, A., Bartolomé, R. A., Vasanji, A., Ambrogio, C., Chiarle, R., Teixidó, J., Risteli, J., Apte, S. S., del Pozo, M. A., and Arroyo, A. G. (2010) MT1-MMP is required for myeloid cell fusion via regulation of Rac1 signaling. *Dev. Cell* **18,** 77–89
51. Satoh, T., Takeuchi, O., Vandenbon, A., Yasuda, K., Tanaka, Y., Kumagai, Y., Miyake, T., Matsushita, K., Okazaki, T., Saitoh, T., Honma, K., Matsuyama, T., Yui, K., Tsujimura, T., *et al.* (2010) The Jmjd3-*Irf4* axis regulates M2 macrophage polarization and host responses against helminth infection. *Nat. Immunol.* **11,** 936–944
52. Maeda, K., Kobayashi, Y., Udagawa, N., Uehara, S., Ishihara, A., Mizoguchi, T., Kikuchi, Y., Takada, I., Kato, S., Kani, S., Nishita, M., Marumo, K., Martin, T. J., Minami, Y., and Takahashi, N. (2012) Wnt5a-Ror2 signaling between osteoblast-lineage cells and osteoclast precursors enhances osteoclastogenesis. *Nat. Med.* **18,** 405–412
53. Zhu, S., Pan, W., Song, X., Liu, Y., Shao, X., Tang, Y., Liang, D., He, D., Wang, H., Liu, W., Shi, Y., Harley, J. B., Shen, N., and Qian, Y. (2012) The microRNA miR-23b suppresses IL-17-associated autoimmune inflammation by targeting TAB2, TAB3 and IKK-α. *Nat. Med.* **18,** 1077–1086